Theoretical studies of the hydrolysis of antibiotics catalyzed by a Metallo-β-lactamase.

C. Meliá, S. Ferrer,* V. Moliner*

Departament de Química Física i Analítica; Universitat Jaume I, 12071 Castellón, Spain

J. Bertrán

Departament de Química; Universitat Autònoma de Barcelona, 08193 Bellaterra, Spain

Keywords: mono zinc metallo-beta-lactamases, MβLs, CphA, imipenen, cefotaxime, reaction mechanism, QM/MM, carbapenem, cephalosporine, free energy profiles

Corresponding authors:

S. Ferrer: sferrer@uji.es

V. Moliner: moliner@uji.es

Abstract

In this paper, hybrid QM/MM molecular dynamics (MD) simulations have been performed to explore the mechanisms of hydrolysis of two antibiotics, Imipenen (IMI), an antibiotic belonging to the subgroup of carbapenems, and the Cefotaxime (CEF), a third-generation cephalosporin antibiotic, in the active site of a mono-nuclear β-lactamase, CphA from Aeromonas hydrophila. According to our results, significant different transition state structures are obtained for the hydrolysis of both antibiotics: while the TS of the CEF is a ionic species with negative charge on nitrogen, the IMI TS presents a tetrahedral-like character with negative charge on oxygen atom of the carbonyl group of the lactam ring. Thus, dramatic conformational changes can take place in the cavity of CphA to accommodate different substrates, which would be the origin of its substrate promiscuity. This feature of the β-lactamase would be in turn, associated to the different mechanisms that the protein employs to hydrolyze the different antibiotics; i.e. the catalytic promiscuity. Since CphA shows only activity against carbapenem antibiotic, this study will be used to shed some light into the origin of the selectivity of the different MbL and, as a consequence, into the discovery of specific and potent MβL inhibitors against a broad spectrum of bacterial pathogens.

Introduction

β-lactam antibiotics are the most effective chemotherapeutic agents for the treatment of bacterial infections, accounting for more than half of the world's antibiotic market.[1,2] The mechanism of the antibacterial activity of β-lactames involves the inhibition of the biosynthesis of the bacterial cell wall peptidoglycan. Nevertheless, despite much progress in antibiotics design has been done during the past decades, the increasing use of these compounds has induced the development of different resistance mechanisms in pathogenic microorganisms.[1] One strategy developed by bacteria to resist the action of antibiotics is the expression of β-lactamases[3] that hydrolyse the four-membered ring of β-lactam antibiotics. It is accepted that hydrolysis involves nucleophilic attack on the carbonyl group of the β-lactam ring and protonation of N atom with concomitant scission of the carbon-nitrogen bond. Nevertheless, there is still a question of debate on the timing of carbon-nitrogen scission bond and the protonation of the N, which could even take place concertedly. A detailed knowledge of the hydrolysis of the four-membered ring of β-lactam antibiotics reaction mechanism is required in order to know the possible ways of inhibiting bacteria activity. Nevertheless, this is not an easy task due to the plethora of different β-lactamases identified up to now. Today, more than 500 β-lactamases are known, classified into four groups,[4] A-D, according to their amino acid sequence.[5] Groups A, C and D, also called serine-β-lactamases (SβLs), utilize an active site serine as a nucleophile,[1] while B group, or metallo-β-lactamases (MβLs), required 1 or 2 Zn(II) ions to perform the hydrolysis.

The MβLs family was defined in 1997 as a new superfamily of metallohydrolases.[6] There has been a growing concern on this zinc-dependent β-lactamases since, despite catalyzing the same reaction, it seems that SβLs and MβLs do not share any structural nor mechanistic similarity[7] and, in fact, the latter are unaffected by all clinically useful inhibitors of the serine-active enzymes.[8] In fact, no MβL inhibitors are available for clinical use.[9]

Three subgroups of MβL have been further identified depending on sequence structure and activity similarities. B1 and B3 subclasses posses a binuclear active site, which requires one or two Zn(II) ions for full activity and are able to hydrolyze carbapenems, pelicinillins and cephalosporins.[9] B2 subclass, unlike those from subclasses B1 and B3, are fully active with one zinc ion bound and possess a narrow spectrum of activity, hydrolyzing carbapenem substrates almost exclusively.[10] Initially, a reduced number of

structures of B2 MβL, CphA from Aeromonas hydrophila,[11] ImiS from Aeromonas veronii bv. Sobria[12] and Sfh-I from Serratia fonticola,[10] have been cristalyzed, being the CphA the most studied one. In particular, three different structures, two of them in the apo form and the last one corresponding to the N220G mutant in complex with a biapenem (Bia) derivative, were obtained. Nevertheless, there are some concerns related with these structures. As commented by Garau et al., the electron density could not be interpreted as either biapenem or a hydrolyzed biapenem molecule, although it was clear the presence of two fused rings near the zinc ion and both, C2 and C3 carbon atoms of the intermediate exhibiting sp3 hybridization.[11] Then, it appears that the molecule has lost the double bond established between these two atoms. Consequently, it is difficult to associate this complex to an intermediate or a product of the antibiotic hydrolysis, as suggested by experimental studies of Sharma et al. for the reaction catalyzed by ImiS.[12] The CphA-Bia complex structure has shown how the zinc metal accommodates in the Zn2 site, with a trigonal bipyramidal coordination formed by Asp120, Cys221, His263, the carboxylate oxygen and the N4 atoms of Bia. Based on these X-ray structures, Garau et al. suggested a mechanism involving a non-metal-binding water nucleophile, activated by His118, that would attack the carbonyl carbon of the substrate, leading to cleavage of the C7-N4 bond of the lactam ring. This proposal has been supported by theoretical calculations of Xu et al.[13,14] although suggesting that Asp120 would be the base activating the water molecule, instead of His118. In a more recent paper, Wu et al. [15] proposed a complete reaction mechanism for the hydrolysis of biapenem antibiotic catalyzed by CphA, arguing that the CphA-Bia complex determined by Garau et al. would belong to a minor pathway, in contrast to the original suggestion. In this regard, simulations performed by Gatti [16] suggest that the bicyclic derivative of Garau et al. would not be formed inside the enzyme active site. Hydrolyzed biapenem might be released first, cyclization would occur in solution and then the bicyclic compound would bind back to the active site.

An alternative mechanism was proposed by Simona et al [17,18] where the nucleophilic attack and the proton transfer to the nitrogen atom of the lactam ring would occur in a single concerted step. According to this proposal, the mechanism requires the activation of a second catalytic water molecule in the active site of the enzyme. This mechanism would be in agreement with experimental studies of Sharma et al [12] based on proton inventories showing that at least one proton transfer must be involved in the rate

limiting step. Nevertheless, the proposal is based on the existence of a conformation of the Michaelis complex in which the substrate binds the zinc metal through a water molecule. This model is not confirmed by the structural studies of Crowder et al.[19] based on enzyme-product complexes, that suggest a direct contact between the zinc metal and the carboxylate of the substrate. An initial structure presenting this direct contact was used by Xu et al.[13-15] to propose a step-wise mechanism that renders an estimated free energy barrier for the nucleophilic attack of ca. 14 kcal·mol^{-1},[13] a value in very good agreement with the kinetic experiments of Garau et al.[11] Nevertheless, this comparison requires the hypothesis that such step was the rate limiting step of the enzymatic cycle, apparently in contradiction with the proton inventory experiments of Crowder et al.[19] and with QM/MM computationally exploration of the full mechanism performed by Simona et al.[17] In particular, the second step related with the proton transfer from Asp120 and Nitrogen atom of substrate, would become the rate limiting step, with a total free energy barrier of ca. 24 kcal·mol^{-1}.

Similar debate was open on the mechanisms of binuclear B1 and B3 beta-lactamases. Thus, Dal Peraro et al.[20] proposed a mechanism with nucleophilic attack and proton transfer taking place in a concerted manner, while the simulations of Xu et al.[21] suggest that the reaction would be essentially stepwise, with a first rate limiting nucleophilic attack leading to an intermediate where the negative charge developed in the nitrogen leaving group would be stabilized by one of the Zn metal atoms (Zn2). This stable anionic intermediate, experimentally reported by Benkovic and co-workers [22] and by Vila and co-workers[23], implies a non-negligible energy barrier for the following step. Again, the studies of Dal Peraro et al, on B1 metallo beta-lactamases assumed an initial structure with the carboxylate of the substrate interacting with the zinc ions through a water molecule. This assumption could be in contradiction with reported X-ray crystallographic structures of the enzyme complex with the hydrolysis product of an antibiotic carried out by Spencer et al. that suggests a direct substrate-metal interaction also in reactant complex.[24]

Interestingly, β-lactamase catalytic activity has been also studied on B1 class with only one zinc metal in the catalytic pocket based on models with the zinc placed in position 1. [20,25,26] The activity of B1 enzymes in their mono-nuclear form has been measured for the hydrolysis of penicillin G catalyzed by Co(II) substitude B1 metallo-β-lactamase, BcII.[27] According to this study, the metal was observed in both positions, 1 and 2.

Furthermore, a biochemical and biophysical characterization of a B3 class of MbL, GOB-18, has also revealed catalytic activity for the mono-nuclear enzyme form with the zinc ion in position 2.

In a previous paper, we carried out a computational study to explore the hydrolysis of one antibiotic, Cefotaxime (CEF), in gas phase and in aqueous solution by means of QM/MM potentials.[28] PM3 semiempirical methods rendered results in qualitative agreement with DFT calculations with B3LYP and M06-2X hybrid functionals. The free energy profiles in solution showed a step-wise mechanism kinetically determined by the nucleophilic attack of a water molecule activated by the proton transfer to the carboxylate group of the substrate (the first step). According the barrier obtained from the second intermediate to products, population of the second intermediate would be in agreement with experimentally detected anionic intermediates in β-lactamases.[22,23] A concerted mechanism, with a water molecule activated by the nitrogen atom of the substrate was also obtained although with a much higher free energy barrier. Keeping in mind the hypothesis that similar molecular mechanisms take place in solution and in the active site of enzymes,[29] we are in this paper exploring these two mechanisms in the active site of a mono- nuclear β-lactamase. In particular, we are studying the hydrolysis of Imipenen (IMI), an antibiotic belonging to the subgroup of carbapenems, and the Cefotaxime (CEF), a third-generation cephalosporin antibiotic, in the active site of CphA from Aeromonas hydrophila (see scheme 1). Keeping in mind that CphA show only activity against carbapenem antibiotic, a comparative analysis of the results obtained for both inhibitors will be used to shed some light into the origin of the selectivity of the different MbL.

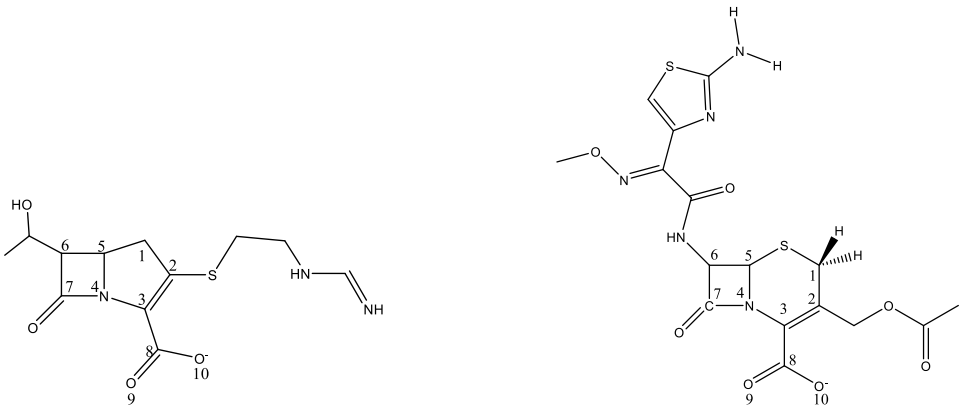

(a) (b)

Scheme 1. Schematic representation of (a) Imipenen, IMI, and (b) Cefotaxime, CEF, β-lactam antibiotics.

Computational Methods

The initial coordinates were taken from the 1.90 Å resolution X-ray crystal structure of a mutated CphA from Aeromonas hydrophila complexed with the hydrolysed biapenem (BMH) antibiotic (PDB entry 1X8I).[11] IMI and CEF were docked on position initially occupied by BMH. Hydrogen atoms were incorporated into the structure to a state complementary to pH 7.5, using fDYNAMO library.[30] Since standard pKa values of ionizable groups can be shifted by local protein environments[31,32], an accurate assignment of the protonation states of all these residues was carried out by recalculating de standard pKa values of the titratable amino acids with the empirical PROPKA3.[33] The residues which have a different pKa from the standard values in solution were: Cys221 unprotonated (with charge of -1); Lys224 defined as neutral; and Glu68 that was defined as protonated. Histidines residues have been protonated as follow: His96 and His263 protonated in N_δ; His 118 and His196 protonated in N_ε; and His176, His268 and His275 protonated in both N (N_δ and N_ε) with a charge of +1. Due to the fact that the total charge of the system was not neutral, four Cl^- counterions were placed in optimal electrostatic positions around the protein (never closer than 10.5 Å from any atom of the system or 5 Å from another counterion, and using a regular grid of 0.5 Å). Then the system was placed in the mass centre of a cavity deleted from a prerelaxed orthorhombic box of water molecules (80 x 80 x 100 $Å^3$). All the water molecules with an oxygen atom lying within 2.8 Å of any heavy atom were removed.

The entire chemical system was then divided into a QM region described by means of PM3[34,35] semiempirical method (using zinc parameters optimized for metalloenzymes[36]), and a MM region described with the OPLS-AA and TIP3P[37] force fields for the protein and water molecules, respectively. The QM region comprised the substrate, the Zinc atom, the side chains of Asn116, His118, Asp120, His196, Cys221 and His 263, and the water molecules that were required for the hydrolysis. The MM region contains the rest of the system, including counterions and crystallization and solvation water molecules. Then, the full system contains 94 QM atoms in the system with IMI and 104 QM atoms in the system with CEF (see Scheme 2). The link-atom method[38] was used to treat the covalent bonds of amino acids crossing the boundary between the QM and MM regions, between the c_α and c_β atoms, to satisfy the valence of the QM fragments.

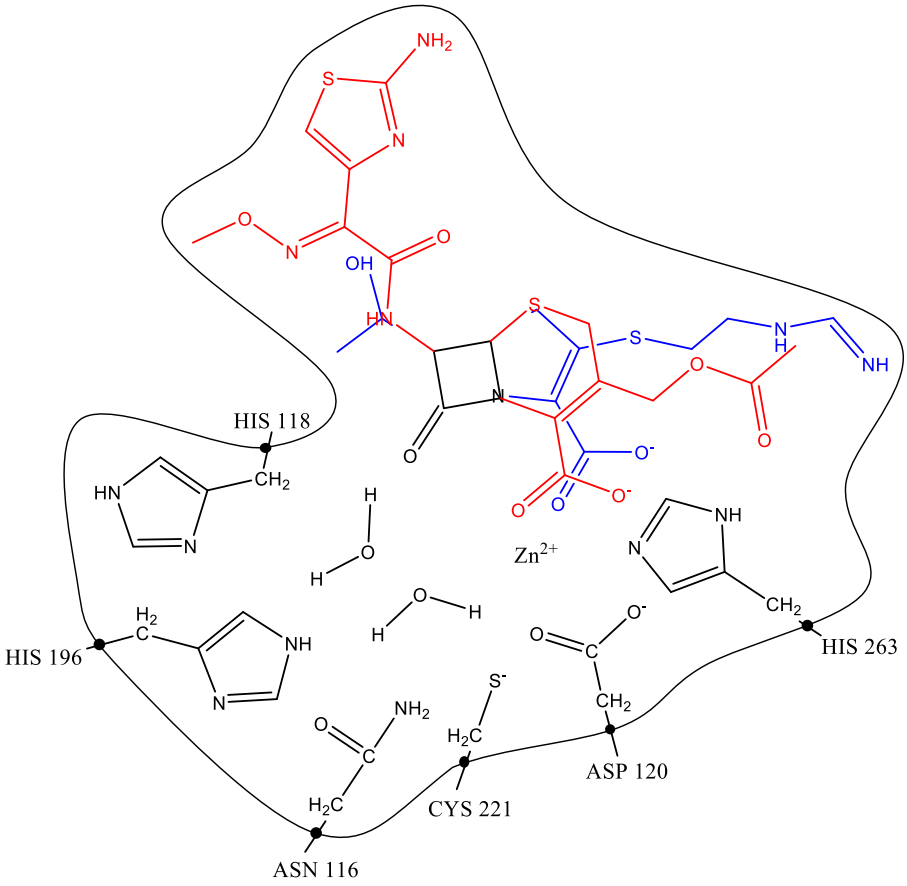

Scheme 2. QM region in the different calculation with Imipenen (IMI in blue) and Cefotaxime (CEF in red), link atoms are represented by black dots.

All atoms away from a sphere of 30 Å radius centered in the substrate, were kept frozen during all simulations. For this purpose, a Langevin bath with a coupling temperature of 300 K was employed throughout this work, using the canonical thermodynamic ensemble (NVT). A total run of 200 ps for the whole system was made with an integration step size of 1 fs. Periodic boundary conditions (PBC) and a switch function of a cutoff distance in the range of 14.5–18 Å were used to treat the nonbonding interactions. After setting up the model, the complete system was optimized using the Adopted Basis Newton Raphson (ABNR) method with the backbone of the protein frozen, and then equilibrated it by 500 ps QM/MM MD simulation.[39] The last structure from this 500 ps MD simulation was fully optimized again to serve as the reaction reactant for the rest of the study. QM/MM Potential Energy Surfaces, PESs, for the four systems have been computed to explore different mechanisms, and stationary point structures characterized by frequency calculations were located. Afterwards, the free energy profiles of the possible reaction paths were obtained in terms of two-dimensional

potential of mean force, 2D PMFs, computed as a function of distinguished geometrical reaction coordinates (RC) deduced from the PESs explorations. In particular, the mechanism found was a concerted mechanism, in particular two RC were chosen, the distance of the nucleophilic attack RC1: d(OH2-C) and the antisymmetric combination of the distances involved in the Nitrogen protonation RC2: d(OH2-H2)-d(H2-N).

The weighted histogram analysis method (WHAM), combined with the umbrella sampling approach,[40,41] was employed to scan the reaction coordinates. Umbrella force constant of 2800 KJ·mol^{-1}·Å^{-2}, were applied to the distinguished reaction coordinates to allow a perfect overlapping among the windows. 10 ps of relaxation and 20 ps of production, with a time step of 0.5 fs using the velocity Verlet algorithm[42] to update the velocities, were run in each window. The PMFs were performed at 300 K, using the NVT ensemble. Structures from the previously obtained QM/MM PESs were used as starting points of each window.

The activation free energy for a particular reaction can be evaluated from the difference in the value of the one dimensional PMF between the maximum (the transition state) and the minimum (the reactants state). The activation free energy can be then recovered from the 2D-PMF tracing a maximum probability reaction path on the 2D-PMF surface and integrating over the perpendicular coordinate. [43]

Because of the large number of structures that must be evaluated during free energy calculations, QM/MM calculations are usually restricted to the use of semiempirical Hamiltonians. In order to reduce the errors associated to the quantum level of theory employed in our simulations, a new energy function defined in terms of interpolated corrections was used:[44-46]

$$E = E_{AM1/MM} + S\left[\Delta E_{LL}^{HL}(\zeta_1,\zeta_2)\right] \qquad (1)$$

where *S* denotes a two-dimensional spline function, and its argument $\Delta E_{LL}^{HL}(\zeta_1,\zeta_2)$ is a correction term evaluated from the single-point energy difference between a high-level (HL) and a low-level (LL) calculation of the QM subsystem. PM3 semiempirical Hamiltonian was used as LL method while a density functional theory (DFT)[47] based

method was selected for the HL energy calculation. In particular, HL energy calculations were performed by means of the hybrid M06-2X[48] functional using the standard 6-31+G* basis set. These calculations were carried out using the *Gaussian09* program.[49]

Results

The reaction paths corresponding to the concerted and the step-wise mechanism, equivalent to the mechanisms previously explored in aqueous solution in our lab,[28] have been explored by QM/MM PESs. The results show that any attempts to get the PESs corresponding to a step-wise mechanism, describing a proton transfer from a water molecule to the oxygen atom of the carboxylate group of the substrate and the nucleophilic attack to the carbonyl carbon of the beta-lactam ring, was unsuccessfully. Obviously, the fact that the carboxylate group is strongly interacting with the Zn ion rules out the possibility of acting as a proton acceptor. The PESs of the concerted mechanism corresponding to the hydrolysis of IMI and CEF are presented in Figure 1. The antisymmetric combination of $O_{w1}H_{w1}$— $H_{w1}N_4$ distances and the O_{w1}— C_7 distances were employed to generate the PESs.

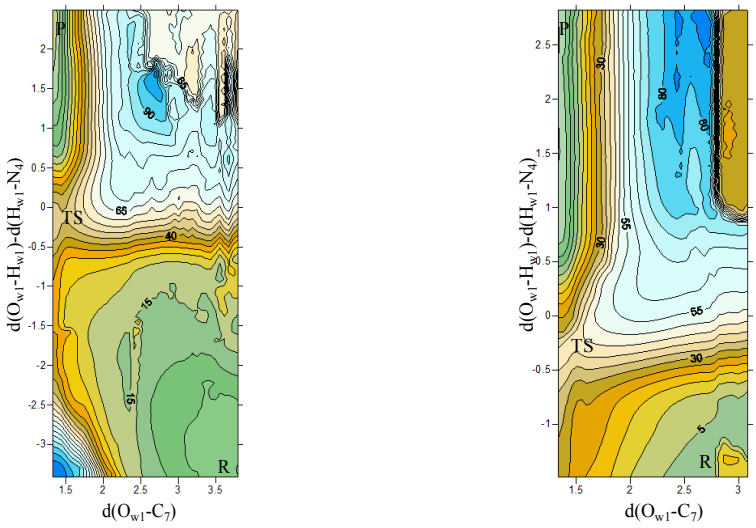

Figure 1. QM/MM PES of hydrolysis of (a) IMI and (b) CEF antibiotics performed in the active site of the CphA from Aeromonas hydrophila.

As observed in Figure 1, the hydrolysis of both antibiotics catalysed by CphA takes place via an asynchronous concerted mechanism. Structures selected from the quadratic region of the saddle point were used to localize and refine the corresponding transition state structures, TSs. Both PESs show how the nucleophilick attack and the proton transfer takes place in a concerted synchronous way from reactants to TS while the process from the TS to products is controlled basically by the coordinate associated to

the proton transfer. IRC paths were traced down from these TSs forward and backwards to the corresponding reactants and products valleys. Finally, fully optimizations were carried out to reach the minimum energy structures, confirming the located TSs connect the reactants and products. Key distances of structures of the active site in reactants, transition states and products are listed in Table S1 of Supporting Information, for hydrolysis of IMI and CEF, respectively.

Once the PESs were explored, the free energy surfaces, obtained in terms of 2D PMFs, were computed and the results are presented in Figure 2. Averaged values of key inter-atomic distances obtained in reactants, TS and products of hydrolysis of both antibiotics are listed in Table 1, schematic representation of these states are presented in Figures 3 and 4, and values of relative energies deduced from the QM/MM 2D PMF and from the PESs, both activation and reaction energies, are listed in Table 2. The free energy surfaces presented in Figure 2 are in a qualitative agreement with the corresponding PESs presented in Figure 1. The minimum free energy profile describes a mechanism where the nucleophilic attack of the water molecule to C7 atom and the proton transfer to the N atom of the beta-lactam ring take place in a concerted way. In both cases, once the TS is reached the process is controlled basically by the coordinate associated to the proton transfer.

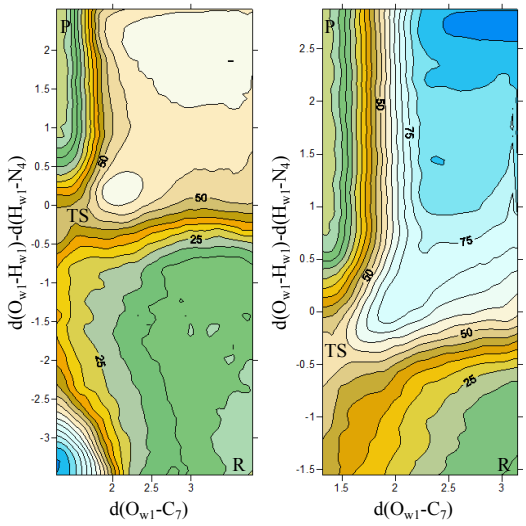

Figure 2. QM/MM 2D PMF of hydrolysis of (a) IMI and (b) CEF antibiotics performed in the active site of the CphA from Aeromonas hydrophila.

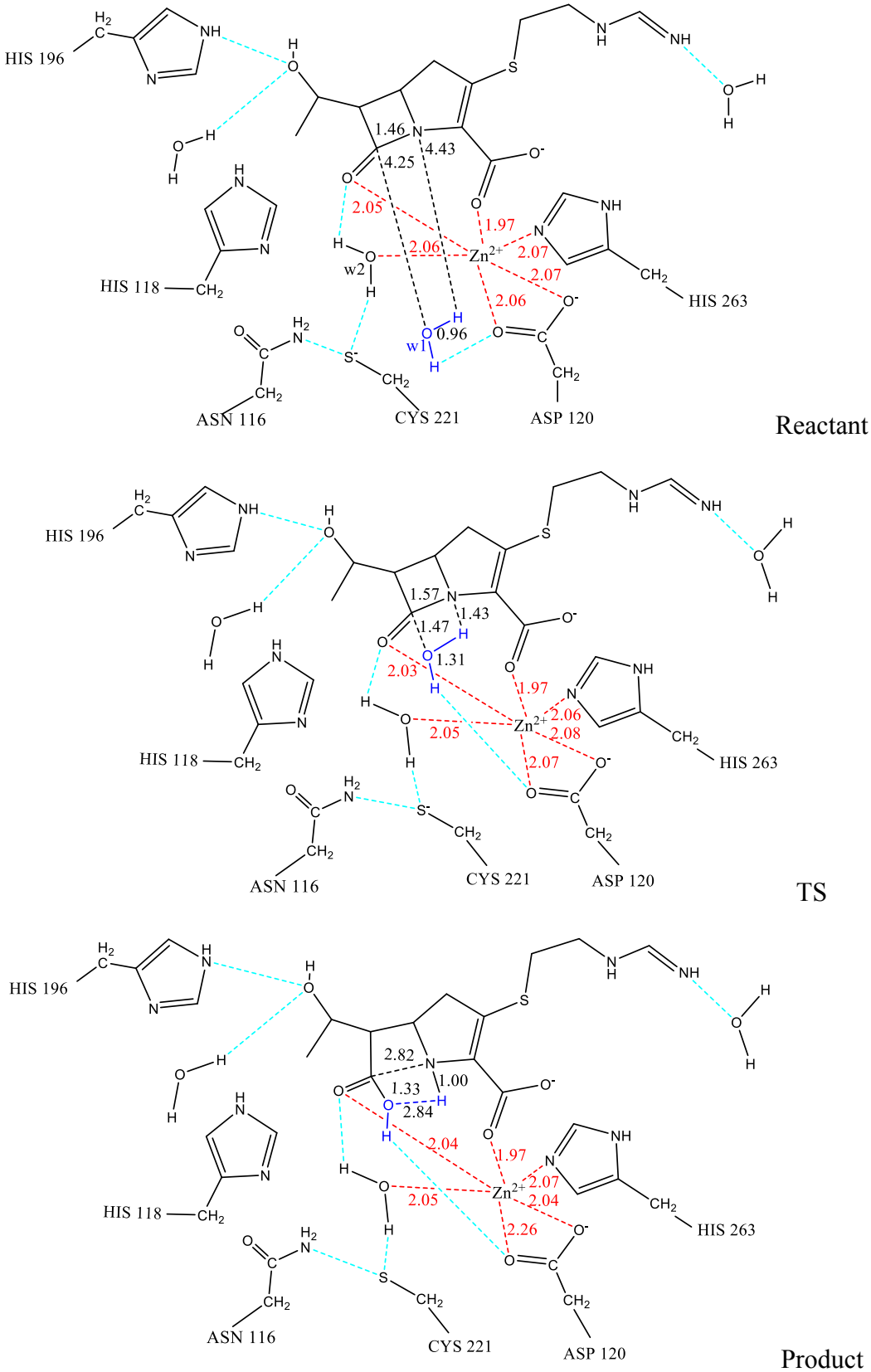

Figure 3. Schematic representation of located structures of reactants, TS and products of the hydrolysis of IMI antibiotics catalysed by the N220G CphA from Aeromonas hydrophila.

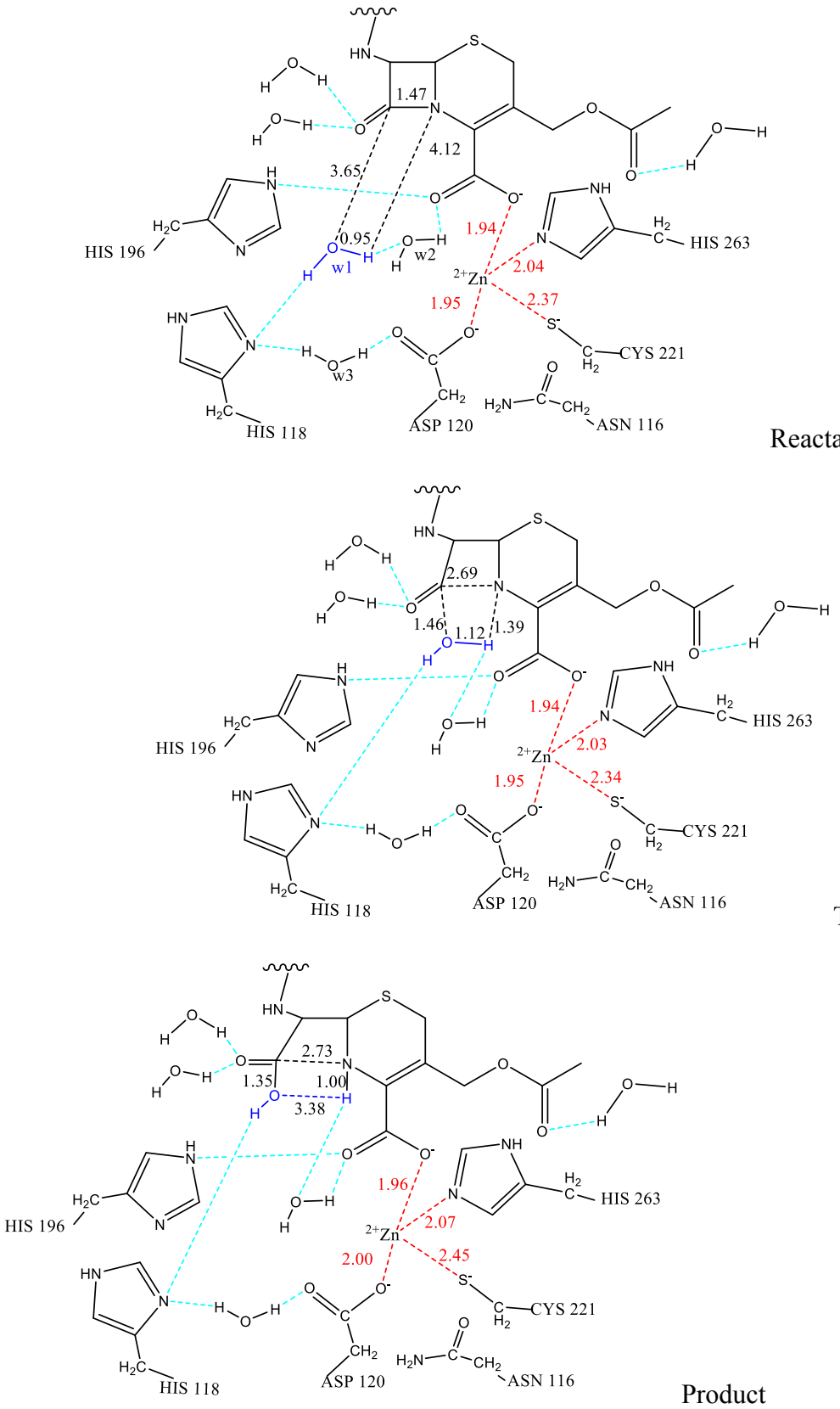

Figure 4. Schematic representation of located structures of reactants, TS and products of the hydrolysis of CEF antibiotics catalysed by the N220G CphA from Aeromonas hydrophila.

As observed in Figure 3, the reactants structure of IMI hydrolysis shows how the Zn appears coordinated to His263, to Asp120 (bifurcated coordination), to a water molecule w2, and to the antibiotic through the carbonyl oxygen and the carboxylate group. The carbonyl bond of IMI seems to be polarized by the water molecule w2 and by the Zn atom, thus activating the C7 atom of the lactam ring for the nucleophilic attack. Another role of w2 molecule is to participate in an indirect coordination between Cys221 and the Zn atom. The reactive water molecule, w1, appears to be oriented by the interaction with Asp120 for the nucleophilic attack to C7. As the reaction proceeds, the w1 molecule approach to the antibiotic and its interaction with Asp120 is lost after reaching the TS. Asp120 interaction with Zn cation does not change during the full process. Nevertheless, while a perfectly symmetric bifurcated interaction is established in reactants and TS of IMI, the Zn ion is preferentially interacting with only one oxygen atom of the Asp120 in products. According to the average values obtained from the structures derived from the 2D PMF, Asp120 would not follow the displacement of the w1 nucleophilic water molecule during the process in IMI hydrolysis. In fact, the shortest distance between oxygen atom of Asp120 and the hydrogen atom of w1 is observed in the TS (1.77 Å) while this distance is significatively larger in products (2.61 Å).

Structures for the hydrolysis of CEF (see Fig. 4) are significantly different. First of all Zn metal presents a tetrahedral coordination, interacting with the carboxylate group of the antibiotic, His263, Cys221 and Asp120. Interestingly, interaction of Asp120 and Zn ion in this system takes place through a single interaction that does not change during the process (from 1.95 to 2.00 Å). The nucleophilic water molecule w1, is interacting with His118 that orients the molecule for the attack, and not with Asp120 as in the IMI hydrolysis. This w1 water molecule is activated by an interaction with the carboxylate group of the substrate through a water molecule w2. Finally, it is also noticeable the interaction between His118 and Asp120 through a conserved water molecule w3. This interaction, as well as the coordination sphere of the Zn atom does not change along the reaction process from reactants to products, as appeared in the IMI hydrolysis reaction.

A detailed analysis of evolution of C7-O distance, as reported in Table 1, shows how the TS in IMI presents a tetrahedral coordination of the C7 carbon atom of the beta lactam ring (1.29 Å), not observed in reactants or products, where the distance is

significantly shorter (1.22 and 1.24 Å, respectively), characteristic of a double bond with a planar conformation. The oxygen atom is basically stabilized by an oxyanion hole through interaction with Zn ion (2.03 Å). The interaction of the carbonyl oxygen established in reactants with the w2 water molecule is stronger than in TS and products, as shown by a shorter interatomic distance (1.79 Å in reactants and 2.40 and 2.43 Å in TS and products, respectively). In CEF hydrolysis, no interaction is observed between O and Zn ion, which is related with the almost unchanged value of C7-O distances during the reaction. The value of the obtained C7-O distance in the three states is characteristic of a double bond (1.20, 1.20 and 1.22 Å in R, TS and products, respectively). These differences are related with the differences observed in the N4-C7 distance. A large value of this distance is observed in the TS of the CEF (2.69 Å) while the value obtained in the IMI TS (1.57 Å) reveals a completely different nature of the TSs. Analysis of the distances describing the position of the transferred proton from the reactive w1 water molecule to N4 atom of the beta-lactam ring shows how the TS of the hydrolysis of IMI is more dissociative than the TS of CEF hydrolysis. Thus, the distances between the transferred proton and the donor and acceptor atoms obtained in IMI (1.31 and 1.43 Å, respectively) are significantly larger than the values obtained in CEF (1.12 Å and 1.39 Å, respectively). These differences of the TS located for the IMI and CEF hydrolysis indicate CphA, depending on the antibiotic, can use different mechanisms.

Population analysis on reactants and TS in both reactions (see Table S2 of Supporting Information) confirms the difference nature of the TSs. The results show how the charge in N4 and carbonyl O atom of the beta-lactam ring are increased by -0.31 a.u. and -0.01 a.u. when going from reactants to TS in the CEF. This trend is completely different in IMI; where the charge on N1 atom is virtually unchanged (from -0.007 to +0.007 a.u.), O atom charge changes from -0.286 to -0.568 a.u. in the TS. As summary, negative charge was located in the O atom of the carbonyl group in the TS of the IMI hydrolysis, while in the CEF the charge is mostly in the N4 atom. This electronic analysis confirms the geometrical analysis and reveals two different mechanisms.

Table 1. Key interatomic distances obtained from the MD simulations performed at reactants, TS and products of the hydrolysis of (a) IMI and (b) CEF antibiotics performed in the active site of the N220G CphA from Aeromonas hydrophila obtained at PM3/MM level. All values are reported in Å.

	IMI			CEF		
	R	TS	P	R	TS	P
d(C7,Ow)	4.25 ± 0.24	1.47 ± 0.00	1.33 ± 0.02	3.65 ± 0.34	1.46 ± 0.00	1.35 ± 0.02
d(Ow,Hw)	0.96 ± 0.02	1.31 ± 0.00	2.84 ± 0.23	0.95 ± 0.02	1.12 ± 0.00	3.38 ± 0.47
d(Hw,N4)	4.43 ± 0.29	1.43 ± 0.00	1.00 ± 0.03	4.12 ± 0.51	1.39 ± 0.00	1.00 ± 0.03
d(C7,N4)	1.46 ± 0.03	1.57 ± 0.00	2.82 ± 0.08	1.47 ± 0.03	2.69 ± 0.00	2.73 ± 0.12
d(O,C7)	1.22 ± 0.02	1.29 ± 0.02	1.24 ± 0.02	1.20 ± 0.02	1.20 ± 0.02	1.22 ± 0.02
d(Zn, O)	2.05 ± 0.05	2.03 ± 0.04	2.04 ± 0.05			
d(Zn, O9)	1.97 ± 0.03	1.97 ± 0.03	1.97 ± 0.03	1.94 ± 0.03	1.94 ± 0.03	1.96 ± 0.03
d(Zn, Asp120-O1)	2.06 ± 0.05	2.07 ± 0.05	2.26 ± 0.41	1.95 ± 0.03	1.95 ± 0.03	2.00 ± 0.05
d(Zn, Asp120-O2)	2.07 ± 0.05	2.08 ± 0.05	2.04 ± 0.05			
d(Zn, His263)	2.07 ± 0.04	2.06 ± 0.04	2.07 ± 0.05	2.04 ± 0.04	2.03 ± 0.04	2.07 ± 0.05
d(Zn, Ow2)	2.06 ± 0.05	2.05 ± 0.04	2.05 ± 0.05			
d(O,Hw2)	1.79 ± 0.11	2.40 ± 0.52	2.43 ± 0.61			
d(Asp120,H2w1)	2.33 ± 0.53	1.77 ± 0.06	2.61 ± 0.54			
d(Zn, Cys221)				2.37 ± 0.08	2.34 ± 0.08	2.45 ± 0.12
d(Hw2-O10)				2.72 ± 0.64	2.04 ± 0.24	2.53 ± 0.53

Table 2. Reaction and activation energies obtained in terms of potential energies ($\Delta E^{\ddagger}$ and ΔE_R) and free energies ($\Delta G^{\ddagger}$ and ΔG_R), for the hydrolysis of IMI and CEF antibiotics performed in the active site of the N220G CphA from Aeromonas hydrophila obtained at PM3/MM and after correction at M06-2X/MM level ($\Delta G^{\ddagger}_{corr}$ and $\Delta G_{R\,corr}$). All values in kcal·mol^{-1}.

	$\Delta E^{\ddagger}$	ΔE_R	$\Delta G^{\ddagger}$	ΔG_R	$\Delta G^{\ddagger}_{corr}$	$\Delta G_{R\,corr}$
IMI	45.5	-9.2	39.2	-6.2	32.6	-9.8
CEF	53.1	-12.9	39.9	-11.2	35.6	-17.5

The reaction and activation energies obtained in terms of potential energies ($\Delta E^{\ddagger}$ and ΔE_R) and free energies ($\Delta G^{\ddagger}$ and ΔG_R), for the hydrolysis of IMI and CEF antibiotics performed in the active site of the N220G CphA from Aeromonas hydrophila obtained at PM3/MM level are reported in Table 2. As observed, both potential energy barriers are quite high, being the reaction of the IMI hydrolysis clearly more favorable (45.5 vs 53.1 kcal·mol^{-1}). Nevertheless, both barriers become almost equivalent when computing the free energy barriers at the same level of theory (39.2 and 39.9 kcal·mol^{-1}, respectively). Thus, a significant reduction in the barriers is observed after including the entropic contribution, more dramatic in the case of the CEF hydrolysis. These values, when including the correction at M06-2X/MM level, are 32.6 and 35.6 kcal/mol^{-1}.

Discussion

Michaelis complex (MC). First conclusion that can be derived from comparison of averaged structures of MC of the hydrolysis reaction of CEF and IMI, with the experimental X-ray diffraction structure is that both MC structures are quite different (see Figure 5). As observed, the structure of CEF in the Michalis complex is similar to the holo-enzyme X-ray structure obtained by Garau et al.[11] The structure of protein complexed with the bis substrate solved by Garau et al., that do not correspond to the reactants; neither an intermediate, is comparable with the structure of MC of CEF obtained after the MD simulations. Also, the experimental results of Garau et al. suggest that the nucleophilic water molecule would be activated by interaction with the His196 residue, as also indicated by our calculations. On the contrary, the MC obtained for the hydrolysis of IMI presents dramatic differences with respect to the experimental structures of the apo or the protein-substrate complex determined by Garau. In particular, the Asp120 interacts in a bifurcated way with the Zn ion, the carbonyl oxygen of the beta lactam ring interacts directly with the Zn ion thus being activated for a nucleophilic attack, and finally, a direct interaction between the metal and the Cys221 is not observed in the structures after our QM/MM MD simulations.

This discussion can be completed by analysis of Figure 5. This figure shows that while the protein backbone of the three structures are almost equivalent, the position of the substrate and the metal ions present differences. Thus, the MC structure of the hydrolysis of CEF (Fig. 5b) is quite similar to the structure of the protein-bis complex deduced from X-ray diffraction methods (Fig. 5a), but the MC structure of the IMI hydrolysis (Fig. 5c) is dramatically different. It seems that the Zn ion is displaced in the

cavity when the protein is complexed with IMI. Moreover, the antibiotic adopts a conformation significantly different to the one observed in the MC of CEF hydrolysis or in the X-ray structure of the protein-bis complex. This can be clearly observed when the structures are overlapped by the backbone of the proteins (Fig. 5d). These structural differences between the MC complexes of IMI and CEF must be related with the different mechanisms observed in both systems. Nevertheless, it is important to point out that, in both cases, the antibiotic is coordinated to the metal that remains anchored to residues such as Asp120 and His263.

Different coordination modes of metal ion in the active site of metalloenzymes has been already observed experimentally by Tawfik and co-workers.[50] This plasticity can be required for the different steps of the full catalytic cycle or it can also promote catalytic promiscuity. In particular, the mechanistic implication of the motion of the zinc ions dizinc metallo-beta-lactamases was already observed by Breece et al.[51] Thus, keeping in mind that the structural experimental evidences are based on the apo enzyme or on a complex not corresponding to the reactants or intermediate, none of the obtained structures could be, a priori, discarded.

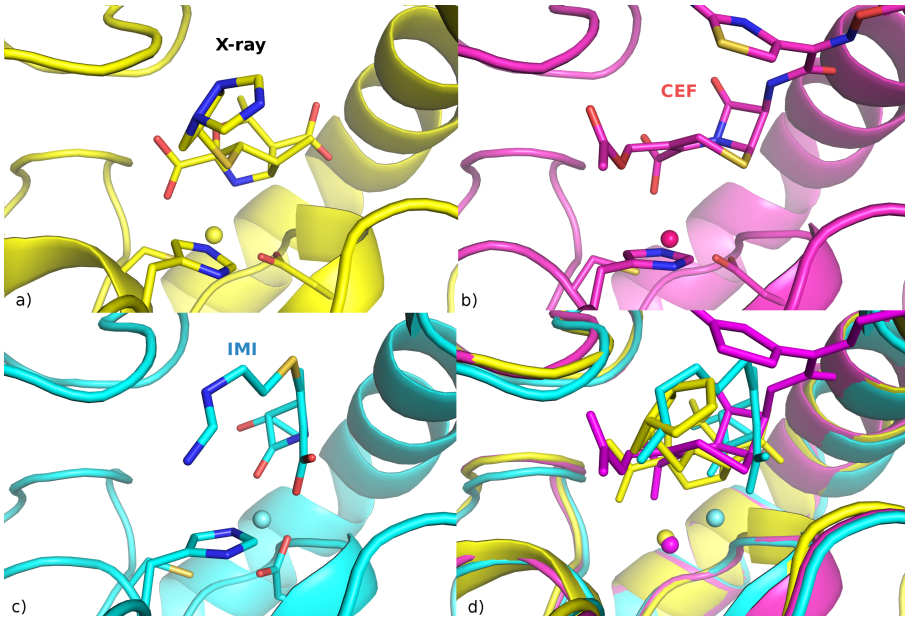

Figure 5. a) X-ray structure of CphA complexed with BMH (PDB entry 1X8I). Representative structures of the Michaelis complex of the hydrolysis of CEF (b) and IMI (c) antibiotics obtained from the QM/MM MD simulations. d) Overlapping of structures presented in panels a, b and c. Hydrogen atoms have been removed in all panels for clarity purposes. Residues Asp120, Cys221 and His263 have been represented by sticks in a, b, and c panels.

The problem related with the plasticity of metal ions in the active site of proteins has been also discussed in enzymes belonging to the Alkaline Phosphatase superfamily, that contains two Zn ions in the active site. Theoretical simulations performed with hybrid QM/MM methods, including specific d-orbital description in the semiempirical AM1 Hamiltonian, was found that movement of Zn ions is dramatic from R to TS.[52-55] . Nevertheless, we must consider the possibility that, as mentioned by Hou and Cui,[56] the main cause for the large structural variations in our simulations[52-55] was the use of AM1 to describe the metal ion. The question of whether the large mobility of the metals in this kind of enzymes is an artifact of the computing methods or reveals the plasticity of the metals in the active site requires further validation to provide a definitive answer, as recently proposed in a perspective paper by Kamerlin and co-workers.[57] In particular, there are no experimental X-ray structures of the Michaelis complex of mono-nuclear metallo-beta-lactamases with different substrates to confirm the observations obtained in the present paper, where the QM/MM MD simulations have been performed using the semiempirical PM3 hamiltonian.

Conclusions

In this paper, hybrid QM/MM molecular dynamics (MD) simulations have been performed to explore the mechanisms of hydrolysis of two antibiotics, IMI (an antibiotic belonging to the subgroup of carbapenems) and CEF (a third-generation cephalosporin antibiotic), catalyzed by a mono-nuclear β-lactamase, CphA from Aeromonas hydrophila. The calculations have allow obtaining, not only the free energy profiles that determines the mechanisms and the energetics of the processes, but also a deep conformational analysis of the active site. Regarding to the two explored mechanism, the hydrolysis of the four-membered ring of β-lactam antibiotics takes place through a concerted mechanism where the nucleophilic attack on the carbonyl group of the β-lactam ring, the protonation of the N atom and scission of the carbon-nitrogen bond take place in a single chemical step. Any attempt to obtain the stepwise mechanism, which is the most favourable reaction path for hydrolysis of these two antibiotics in aqueous solution[28] was unsuccessful. A deeper comparative analysis of the two reactions in CphA reveals electronically different transition state structures: while

the TS of the CEF is a ionic species with negative charge on nitrogen, the IMI TS presents a tetrahedral-like character with negative charge on oxygen atom of the carbonyl group of the lactam ring. According to our results, dramatic conformational changes can take place in the cavity of CphA to accommodate different substrates, which would be the origin of its substrate promiscuity. This feature of the β-lactamase would be in turn, associated to the different mechanisms that the protein employs to hydrolyze the different antibiotics; i.e. the catalytic promiscuity.

From the energetic point of view, the PMFs obtained at the highest level of theory used in the present study, when including the correction at M06-2X/MM level, render free energy barriers of 32.6 and 35.6 kcal/mol^{-1} for the hydrolysis of IMI and CEF, respectively. This trend would be in agreement with the fact that CphA shows only activity against carbapenem antibiotic. Nevertheless, in our previous study in aqueous solution,[28] a substrate assisted mechanism presented a barrier of 30.8 kcal·mol^{-1} at M06-2X/MM level. Then, although possible, the explored mechanism does not seem to be the one taking place in the mono metallo-β-lactamase proteins, considering the obtained free energy barriers in both media. Our results suggest that the protein could have a chemical role in the catalytic process by favoring the reaction to progress through the existence of an intermediate. This is in agreement with a two-step mechanism involving participation of a water molecule, as proposed by Simona et al.,[18] Asp120 as proposed by Wu et al.,[15] or His196 as suggested by Garau et al.[11] Our results, together with these previous studies, demonstrate the complexity of the enzyme reaction mechanisms in mono metallo-β-lactamases. In most of the cases, reaction coordinate would involve participation of the environment and further more complex explorations of free energy surfaces would be required. The complete computational study will then be used to shed some light into the origin of the selectivity of the different MβL and, as a consequence, into the discovery of specific, potent MβL inhibitors against a broad spectrum of bacterial pathogens.

Acknowledgements

This work was supported by the Spanish *Ministerio de Economía y Competitividad* for project CTQ2012-36253-C03; *Generalitat Valenciana* for Prometeo/2009/053 project,

and Universitat Jaume I for project P1·1B2011-23. The authors also acknowledge the Servei d´Informatica, Universitat Jaume I for generous allotment of computer time.

References.

1. J. F. Fisher; S. O. Meroueh; S. Mobashery. Chem Rev **2005**, *105*, 395-424.

2. P. E. Tomatis; R. M. Rasia; L. Segovia; A. J. Vila. Proc Natl Acad Sci U S A **2005**, *102*, 13761-13766.

3. Y. Yamaguchi; T. Kuroki; H. Yasuzawa; T. Higashi; W. C. Jin; A. Kawanami; Y. Yamagata; Y. Arakawa; M. Goto; H. Kurosaki. J Biol Chem **2005**, *280*, 20824-20832.

4. T. R. Walsh; M. A. Toleman; L. Poirel; P. Nordmann. Clin Microbiol Rev **2005**, *18*, 306-325.

5. R. P. Ambler. Philosophical Transactions of the Royal Society of London B, Biological Sciences **1980**, *289*, 321-331.

6. A. F. Neuwald; J. S. Liu; D. J. Lipman; C. E. Lawrence. Nucleic Acids Res **1997**, *25*, 1665-1677.

7. J. M. Gonzalez; F. J. M. Martin; A. L. Costello; D. L. Tierney; A. J. Vila. J Mol Biol **2007**, *373*, 1141-1156.

8. J. H. Toney; P. M. D. Fitzgerald; N. Grover-Sharma; S. H. Olson; W. J. May; J. G. Sundelof; D. E. Vanderwall; K. A. Cleary; S. K. Grant; J. K. Wu; J. W. Kozarich; D. L. Pompliano; G. G. Hammond. Chem Biol **1998**, *5*, 185-196.

9. P. Oelschlaeger; N. Ai; K. T. DuPrez; W. J. Welsh; J. H. Toney. J Med Chem **2010**, *53*, 3013-3027.

10. F. Fonseca; E. H. C. Bromley; M. J. Saavedra; A. Correia; J. Spencer. J Mol Biol **2011**, *411*, 951-959.

11. G. Garau; C. Bebrone; C. Anne; M. Galleni; J. M. Frere; O. Dideberg. J Mol Biol **2005**, *345*, 785-795.

12. N. P. Sharma; C. Hajdin; S. Chandrasekar; B. Bennett; K.-W. Yang; M. W. Crowder. Biochemistry **2006**, *45*, 10729-10738.

13. D. Xu; D. Xie; H. Guo. J Biol Chem **2006**, *281*, 8740-8747.

14. D. Xu; Y. Zhou; D. Xie; H. Guo. J Med Chem **2005**, *48*, 6679-6689.

15. S. S. Wu; D. G. Xu; H. Guo. J Am Chem Soc **2010**, *132*, 17986-17988.

16. D. L. Gatti. PLoS One **2012**, *7*, e30079.

17. F. Simona; A. Magistrato; M. Dal Peraro; A. Cavalli; A. J. Vila; P. Carloni. J Biol Chem **2009**, *284*, 28164-28171.

18. F. Simona; A. Magistrato; D. M. A. Vera; G. Garau; A. J. Vila; P. Carloni. Proteins: Struct, Funct, Bioinf **2007**, *69*, 595-605.

19. M. W. Crowder; J. Spencer; A. J. Vila. Accounts Chem Res **2006**, *39*, 721-728.

20. M. Dal Peraro; A. J. Vila; P. Carloni; M. L. Klein. J Am Chem Soc **2007**, *129*, 2808-2816.

21. D. Xu; H. Guo; G. Cui. J Am Chem Soc **2007**, *129*, 10814-10822.

22. Z. G. Wang; W. Fast; S. J. Benkovic. Biochemistry **1999**, *38*, 10013-10023.

23. M. F. Tioni; L. I. Llarrull; A. s. A. Poeylaut-Palena; M. A. MartiÌ□; M. Saggu; G. R. Periyannan; E. G. Mata; B. Bennett; D. H. Murgida; A. J. Vila. J Am Chem Soc **2008**, *130*, 15852-15863.

24. J. Spencer; J. Read; R. B. Sessions; S. Howell; G. M. Blackburn; S. J. Gamblin. J Am Chem Soc **2005**, *127*, 14439-14444.

25. M. Dal Peraro; L. I. Llarrull; U. Rothlisberger; A. J. Vila; P. Carloni. J Am Chem Soc **2004**, *126*, 12661-12668.

26. M. Dal Peraro; A. J. Vila; P. Carloni. Proteins **2004**, *54*, 412-423.

27. L. I. Llarrull; M. F. Tioni; A. J. Vila. J Am Chem Soc **2008**, *130*, 15842-15851.

28. C. Meliá; S. Ferrer; V. Moliner; I. Tuñón; J. Bertrán. J Comput Chem **2012**, *33*, 1948-1959.

29. A. Warshel. Computer modeling of chemical reactions in enzymes and solutions; Wiley: New York, 1991.

30. M. J. Field; M. Albe; C. Bret; F. Proust-De Martin; A. Thomas. J Comp Chem **2000**, *21*, 1088-1100.

31. S. Ferrer; E. Silla; I. Tuñón; M. Oliva; V. Moliner; I. H. Williams. Chem Commun (Cambridge, U K) **2005**, 5873-5875.

32. J. Antosiewicz; J. A. McCammon; M. K. Gilson. J Mol Biol **1994**, *238*, 415-436.

33. M. H. M. Olsson; C. R. Sondergaard; M. Rostkowski; J. H. Jensen. J Chem Theor Comput **2011**, *7*, 525-537.

34. J. J. P. Stewart. J Comput Chem **1989**, *10*, 221-264.

35. J. J. P. Stewart. J Comput Chem **1989**, *10*, 209-220.

36. E. N. Brothers; D. Suarez; D. W. Deerfield; K. M. Merz. J Comput Chem **2004**, *25*, 1677-1692.

37. W. L. Jorgensen; J. Chandrasekhar; J. D. Madura; R. W. Impey; M. L. Klein. J Chem Phys **1983**, *79*, 926-935.

38. U. C. Singh; P. A. Kollman. J Comput Chem **1986**, *7*, 718-730.

39. L. Verlet. Physical Review **1967**, *159*, 98-103.

40. S. Kumar; D. Bouzida; R. H. Swendsen; P. A. Kollman; J. M. Rosenberg. J Comp Chem **1992**, *13*, 1011-1021.

41. G. M. Torrie; J. P. Valleau. J Comp Phys **1977**, *23*, 187-199.

42. L. Verlet. Phys Rev **1967**, *159*, 98-103.

43. G. K. Schenter; B. C. Garrett; D. G. Truhlar. J Chem Phys **2003**, *119*, 5828-5833.

44. J. J. Ruiz-Pernía; E. Silla; I. Tuñón; S. Martí. J Phys Chem B **2006**, *110*, 17663-17670.

45. Y. Y. Chuang; J. C. Corchado; D. G. Truhlar. J Phys Chem A **1999**, *103*, 1140-1149.

46. S. Ferrer; S. Martí; V. Moliner; I. Tuñón; J. Bertran. Phys Chem Chem Phys **2012**, *14*, 3482-3489.

47. W. Kohn; A. D. Becke; R. G. Parr. J Phys Chem **1996**, *100*, 12974-12980.

48. Y. Zhao; D. G. Truhlar. Theor Chem Acc **2008**, *120*, 215-241.

49. Gaussian 09. Revision A.1 M. J. Frisch; G. W. Trucks; H. B. Schlegel; G. E. Scuseria; M. A. Robb; J. R. Cheeseman; G. Scalmani; V. Barone; B. Mennucci; G. A. Petersson; H. C. Nakatsuji, M.; Li, X.; Hratchian, H. P.; Izmaylov, A. F.; Bloino, J.; Zheng, G.; Sonnenberg, J. L.; Hada, M.; Ehara, M.; Toyota, K.; Fukuda, R.; Hasegawa, J.; Ishida, M.; Nakajima, T.; Honda, Y.; Kitao, O.; Nakai, H.; Vreven, T.; Montgomery, Jr., J. A.; Peralta, J. E.; Ogliaro, F.; Bearpark, M.; Heyd, J. J.; Brothers, E.; Kudin, K. N.; Staroverov, V. N.; Kobayashi, R.; Normand, J.; Raghavachari, K.; Rendell, A.; Burant, J. C.; Iyengar, S. S.; Tomasi, J.; Cossi, M.; Rega, N.; Millam, N. J.; Klene, M.; Knox, J. E.; Cross, J. B.; Bakken, V.; Adamo, C.; Jaramillo, J.; Gomperts, R.; Stratmann, R. E.; Yazyev, O.; Austin, A. J.; Cammi, R.; Pomelli, C.; Ochterski, J. W.; Martin, R. L.; Morokuma, K.; Zakrzewski, V. G.; Voth, G. A.; Salvador, P.; Dannenberg, J. J.; Dapprich, S.; Daniels, A. D.; Farkas, Ö.; Foresman, J. B.; Ortiz, J. V.; Cioslowski, J.; Fox, D. J. Gaussian Inc. Wallingford CT **2009**

50. M. Ben-David; G. Wieczorek; M. Elias; I. Silman; J. L. Sussman; D. S. Tawfik. J Mol Biol **2013**, *425*, 1028-1038.

51. R. M. Breece; Z. Hu; B. Bennett; M. W. Crowder; D. L. Tierney. J Am Chem Soc **2009**, *131*, 11642-11643.

52. V. López-Canut; M. Roca; J. Bertran; V. Moliner; I. Tuñón. J Am Chem Soc **2011**, *133*, 12050-12062.

53. V. López-Canut; M. Roca; J. Bertran; V. Moliner; I. Tuñón. J Am Chem Soc **2010**, *132*, 6955-6963.

54. V. López-Canut; S. Martí; J. Bertran; V. Moliner; I. Tuñón. J Phys Chem B **2009**, *113*, 7816-7824.

55. K. Y. Wong; J. Gao. Biochemistry **2007**, *46*, 13352-13369.

56. G. Hou; Q. Cui. J Am Chem Soc **2012**, *134*, 229-246.

57. F. Duarte; B. A. Amrein; S. C. L. Kamerlin. Phys Chem Chem Phys **2013**, *15*, 11160-11177.